

**Figure 3** Concentrations of PCBs, classed by number of chlorine atoms per molecule in snow from four of the study sites. Vapour pressures decrease with increasing chlorination (Table 1). We note the increase in the more-volatile, less-chlorinated PCBs at high elevation. Similar tendencies have been shown in lake sediments along latitudinal gradients<sup>14</sup>. Dichlorobiphenyls are PCB numbers 6,8/5; tri-17,18,19,16/32,24/27,22,25,26,28,31,33; tetra-41/47,40,42,44,45,46,47,48,49,52,56/60,64,70/76,74,82; penta-83,84/89,85,91,97,99,101,105,110,114,118; hexa-128,130/176,131,132,134,136,137,138,141,146,144/135,149,151,153,158; hepta-174,175,177,179,178/129,183,185,187.

higher elevations. For example, cities like Denver and Mexico City derive their water supply from snowmelt on mountains over 3,000 m high. They are also much closer to industrial and agricultural sources of contaminants in areas that reach summer temperatures 5–10 °C warmer than those of western Canada. The effect of cold condensation on the fate of organochlorine in these areas remains unknown, but is likely to result in more pronounced accumulation of toxic compounds than we have observed in our study area. □

Received 9 January; accepted 21 July 1998.

- Donald, D. B. *et al.* Polychlorinated Biphenyls and Organochlorine Pesticides in the Aquatic Environment along the Continental Divide Region of Alberta and British Columbia (Spec. Rep. Inland Waters Directorate, Environment Canada, Regina, Saskatchewan, 1993).
- Welch, H. E. *et al.* Brown snow: a long-range transport event in the Canadian Arctic. *Environ. Sci. Technol.* **25**, 280–286 (1991).
- Wania, F. & Mackay, D. Global fractionation and cold condensation of low volatility organochlorine compounds in polar regions. *Ambio* **22**, 10–18 (1993).
- Simonich, S. L. & Hites, R. A. Global distribution of persistent organochlorine compounds. *Science* **269**, 1851–1854 (1995).
- Miskimmin, B. *et al.* Chlorobornanes in sediments and fish thirty years after toxaphen treatment of lakes. *Environ. Sci. Technol.* **29**, 2490–2495 (1995).
- Campbell, L. M. *The Use of Stable Isotope Ratios to Discern Organochlorine Bioaccumulation Patterns in a Sub-alpine Rocky Mountain Lake Food Web*. Thesis, Univ. Alberta (1997).
- Kidd, K. A. *et al.* High toxaphene concentrations in fish from a subarctic lake. *Science* **269**, 240–242 (1995).
- Kidd, K. A. *et al.* Correlation between stable nitrogen isotope ratios and concentrations of organochlorines in biota from a freshwater food web. *Sci. Tot. Environ.* **160/161**, 381–390 (1995).
- Weathers, K. C. *et al.* A regional acidic/fog water event in the eastern United States. *Nature* **319**, 657–658 (1986).
- Baltensperger, U. *et al.* Transfer of atmospheric constituents into an alpine snow field. *Atmos. Environ.* **A 27**, 1881–1890 (1993).
- Muir, D. C. G. *et al.* Organochlorine contaminants in arctic marine food chains: accumulation of specific polychlorinated biphenyls and chlordane-related compounds. *Environ. Sci. Technol.* **22**, 1071–1079 (1988).
- Muir, D. C. G. *et al.* Spatial trends and historical profiles of organochlorine pesticides in Arctic lake sediments. *Sci. Tot. Environ.* **160/161**, 447–457 (1995).
- Hinckley, D. A. *et al.* Determination of vapor pressures for nonpolar and semipolar organic compounds from gas chromatographic retention data. *J. Chem. Eng. Data* **35**, 323–327 (1990).
- Muir, D. C. G. *et al.* Spatial trends and historical deposition of polychlorinated biphenyls in Canadian mid-latitude and arctic lake sediments. *Environ. Sci. Technol.* **30**, 3609–3617 (1996).
- Muir, D. C. G. *et al.* Geographic variation of chlorinated hydrocarbons in burbot (*Lota lota*) from remote lakes and rivers in Canada. *Arch. Environ. Contam. Toxicol.* **19**, 530–542 (1990).
- Gregor, D. J. in *Seasonal Snowpacks* (ed. Davies, T.) 323–358 (NATO Ser. G, Vol. 28, Springer, Berlin, 1991).
- Wania, F. Modelling the fate of non-polar organic chemicals in an aging snowpack. *Chemosphere* **35**,

2345–2363 (1997).

- Metcalf, R. L. *Organic Insecticides, their Chemistry and Mode of Action* (Interscience, New York, 1955).
- Canadian Arctic Contaminant Assessment Report (Minister of Public Works and Government Services, Ottawa, Canada, 1997).
- Schindler, D. W. & Pacas, C. in *Ecological Outlooks Project* (eds Green, J., Pacas, C., Bayley, S. & Cornwall, L.) (Banff-Bow Valley Study, Dept of Canadian Heritage, Ottawa, 1996).
- Mackay, D., Shiu, W. Y. & Ma, K.-C. *Illustrated Handbook of Physical-Chemical Properties and Environmental Fate for Organic Chemicals Vol. V* (Lewis Publishers, Boca Raton, FL, 1997).
- Mackay, D., Shiu, W. Y. & Ma, K.-C. *Illustrated Handbook of Physical-Chemical Properties and Environmental Fate for Organic Chemicals Vol. 1. Monoaromatic Hydrocarbons Chlorobenzenes and PCBs* (Lewis Publishers, Chelsea, Michigan, 1992).

**Acknowledgements.** We are grateful to the Banff Warden Office, in particular D. Gilbride, for help with locating weather stations and providing meteorological data. We thank the ski patrol crews from Lake Louise, Sunshine, Tod and Whistler ski mountains for their support and interest. Sample fractionation and GC analyses were conducted at the Freshwater Institute, Winnipeg. R. Crosley and L. Mottle from Environment Canada, Calgary, supplied expertise, sampling equipment and laboratory facilities for this work. This work was supported by the Canadian Chlorine Coordinating Committee (C4), an NSERC Strategic Grant, and an NSERC Operating Grant (D.W.S.).

Correspondence and requests for materials should be addressed to J.M.B. at the University of Ottawa (e-mail: blais@science.uottawa.ca).

## The influence of natural mineral coatings on feldspar weathering

M. A. Nugent\*†, S. L. Brantley\*, C. G. Pantano‡ & P. A. Maurice§

\* Department of Geosciences, ‡ Department of Material Science and Engineering, The Pennsylvania State University, University Park, Pennsylvania 16802, USA  
§ Department of Geology, Kent State University, Kent, Ohio 44242, USA

Quantification of the rate of weathering of feldspar, the most abundant mineral in the Earth's crust, is required to estimate accurately carbon dioxide fluxes over geological timescales and to model groundwater chemistry. Laboratory dissolution rates, however, are consistently found to be up to four orders of magnitude higher than the 'natural' rates<sup>1,2</sup> measured in the field. Although this discrepancy has been attributed to several factors<sup>3</sup>, previous research has tended to suggest that the underlying mechanism of feldspar dissolution under acidic pH may differ between the field and the laboratory<sup>3</sup>. Here we demonstrate that weathered albite surfaces, like laboratory-dissolved samples, are sodium- and aluminium-depleted, indicating that the dissolution mechanism in acidic soils is similar to that in acidic laboratory solutions. We find that microtopography images are consistent with dissolution occurring at specific surface sites—indicative of surface-controlled dissolution dominated by a non-stoichiometric layer. Elevated aluminium and silicon ratios reported previously<sup>3,4</sup>, and used to suggest a mechanism for field weathering different from laboratory dissolution<sup>3</sup>, can alternatively be explained by a thin, hydrous, patchy, natural coating of amorphous and crystalline aluminosilicate. This coating, which is largely undetected under scanning electron microscopy after cleaning, but visible under atomic force microscopy, alters surface chemistry measurements and may partially inhibit the field dissolution rate.

Numerous laboratory dissolution studies on feldspar at acidic pH reveal Na/Ca/K- and Al-depleted surfaces, as documented by X-ray photoelectron spectroscopy (XPS)<sup>5–10</sup>, secondary ion mass spectrometry (SIMS)<sup>6,8,9,11,12</sup> and other techniques<sup>13–18</sup>. Depleted surfaces have been used to suggest that the mechanism of feldspar dissolution in the laboratory involves detachment of an Al-depleted, H-enriched surface complex<sup>14,17,18</sup>. In contrast, Al depletion on naturally weathered feldspar has never been reported. Instead, either elevated Al/Si ratios<sup>3,4</sup> or Al/Si ratios unaltered from the

† Present address: Department of Geosciences, SUNY at Stony Brook, Stony Brook, New York 11794-2100, USA.

bulk<sup>19</sup> are reported for feldspars from acidic soils. Nesbitt and Muir<sup>3</sup> inter that the surface Al/Si enrichment of oligoclase removed from a 10,000-year-old Canadian (acidic) spodosol is due to Si depletion, which implies that the dissolution mechanism differs from that in the laboratory.

To assess the mechanism of feldspar dissolution in an acidic soil, albite tablets (Ab<sub>90</sub>An<sub>10</sub>, which is 90 mol% albite, 10 mol% anorthite) from Havre de Grace, Quebec, were polished to 0.25 μm on the (001) cleavage face and buried in the B horizon of a spodosol (State College, Pennsylvania). The 'albite' samples are peristerites (alternating albite and oligoclase lamellae) with a bulk composition within the albite compositional range. Several holey bottles containing albite tablets and soil were buried in August 1993, and one bottle was removed after 0.5, 1, 2, 3 and 3.5 years. Upon retrieval, the 6-month, 1- and 2-year samples were briefly rinsed in water then ultrasonicated in acetone. The 3- and 3.5-year tablets were ultrasonicated in high-purity acetone for 20 and 45 min, respectively, and stored in a desiccator. Polished unweathered blanks were prepared and left unweathered in the desiccator.

The burial site is located in a humid, temperate climate, which is vegetated by conifers and receives 103 cm of acidic (pH 4.3) precipitation annually. The B horizon (quartz, minor kaolinite and minor iron oxides) is overlain by a thin (<5 cm), organic-rich A horizon. Soil pore waters, sampled at burial depth by suction lysimeter in 1995–96 varied in pH from 4.9 to 5.6 (average, 5.1) and were under- and supersaturated with respect to all feldspars and kaolinite, respectively.

Surface microtopography (Fig. 1), which is not present before burial, indicates that dissolution occurred during weathering. Etching of specific surface sites, as observed under Tapping Mode atomic force microscopy (AFM) is consistent with a surface-controlled dissolution mechanism, in agreement with previous scanning electron microscope (SEM) observations for naturally weathered and laboratory-dissolved feldspars<sup>20–22</sup>. Based on microtopography development over 3 years, our field dissolution rate<sup>23</sup>, estimated between 10<sup>-16</sup> and 10<sup>-18</sup> mol<sub>feldspar</sub> cm<sup>-2</sup> s<sup>-1</sup> is comparable

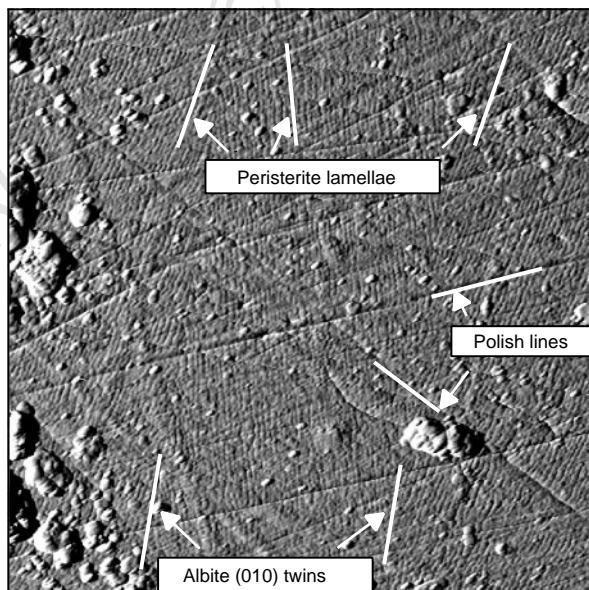


**Figure 1** Tapping Mode instrument AFM amplitude image (2.5 × 2.5 μm) in a coating-free area of peristeritic albite weathered for 3 years. The microtopography is the result of preferential etching of albite (010) twins and albite and oligoclase lamellae, as confirmed by TEM analysis. This microtopography, absent on unweathered samples and never observed under SEM, is present in patches on the sample weathered for 6 months, and everywhere imaged on the 3- and 3.5-year samples. The grooves created by the peristerite lamellae are at least 1.5 nm deep, on average<sup>21</sup>, and polish lines are present before and after weathering.

to other reported field rates<sup>2</sup>, suggesting that our samples dissolved similarly to feldspars weathering naturally.

Using SIMS profiling, no difference in the Al/Si ratio is observed between the unweathered and 6-month samples, but the Al/Si ratio is increased at least 500 Å into the feldspar surface weathered for 1 year (Fig. 2a). Our 1-year profiles are similar to SIMS profiles<sup>3</sup> for oligoclase naturally weathered in an acidic spodosol. XPS analyses (Fig. 3) reveal that the 6-month sample is Al-depleted, but that samples weathered longer than 6 months are Al-enriched. Every weathered albite surface is Na-deficient.

We find that a patchy coating, consisting of particles ranging in size from nanometres to millimetres and in thickness from ~5 nm to 1 μm, covers at least 35% of the 3-year sample after cleaning, as imaged under AFM. This coating, largely undetected under SEM but obvious under AFM, is sufficiently thick to affect XPS (upper ~80 Å) and SIMS (depth profiling) signals. The Na- and Al-depleted 6-month sample has significantly less coating, as observed under AFM.

Sufficient coating coverage will result in higher Al/Si and lower Na/Si ratios than those for unweathered feldspar. The coating, analysed by energy dispersive X-ray analysis (EDX) during transmission electron microscopy (TEM), contains crystalline kaolinite, which has a higher Al/Si and lower Na/Si ratio than albite, in discrete patches within the otherwise amorphous coating material. Amorphous portions of the coating are hydrous (Fig. 2b) and contain Al, Si, O and minor Fe. Because the 6-month sample shows Al and Na depletion and has less coating material, we argue

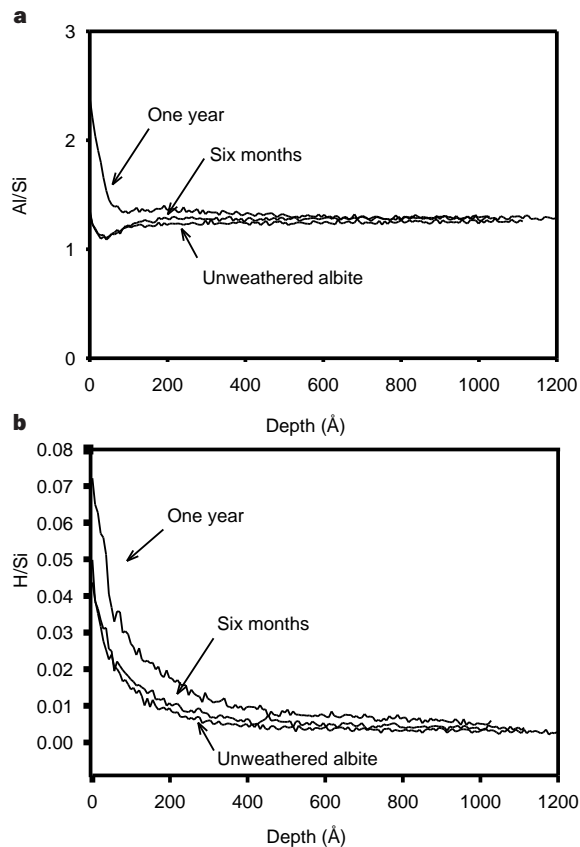


**Figure 2.** SIMS signal ratios as a function of depth into the albite surface. **a**, Al/Si; **b**, H/Si. After gold-coating the samples, a gold-coated TEM grid was laid over the area to be analysed, to provide sufficient charge stabilization during analysis. SIMS profiles were then collected on a Cameca Model IMS/3F using a 50 nA, 15.4 eV, negative O-18 primary beam. The ~75-μm beam was rastered over a 250 × 250 μm area, and positive secondary ions were collected from an area in the centre of the crater which was ~10 μm in diameter. Because AFM analyses reveal that the coating is patchy, coating thickness cannot accurately be assessed by only our SIMS data.

that the albite surface during weathering, like laboratory-dissolved surfaces, is Al- and Na-depleted. A natural coating obscures the feldspar surface XPS and SIMS signals on our other field-weathered samples, because these signals average the Al and Si compositions over coated and uncoated areas of the surface.

A 3.5-year sample, ultrasonicated for 45 min within 1 day of retrieval, revealed relatively low Al/Si (0.32) and Na/Si (0.11) atomic ratios under XPS. Under AFM, the coating coverage on this 3.5-year sample was significantly less than on the 3-year sample. The Na- and Al-depleted signal on this 3.5-year sample, which presumably includes areas covered by coating during weathering, suggests the feldspar surface is Na- and Al-depleted underneath the coating during weathering.

The 3-year sample was ultrasonicated for an additional 20 min, 9 months after retrieval, and re-analysed by XPS. The Al/Si atomic ratio remained high (0.47), the Na/Si ratio remained low (0.08), and the coating coverage under AFM remained approximately the same. The difficulty in removing the coating from the 3-year sample several months after retrieval, and the ease with which coating is removed from the 3.5-year sample immediately after recovery, is consistent with ageing into an adherent layer.

A second set of five samples, buried later and recovered after 1, 2 (2 samples), 3, and 4 months, reveal variable but elevated Al/Si atomic ratios (0.40, 0.40 and 0.51, 0.38, and 0.48, respectively) under XPS, demonstrating that the coating is established very early in weathering. Furthermore, coating removal is difficult and not necessarily reproducible. For example, the two 2-month samples, which were cleaned identically, have Al/Si ratios of 0.40 and 0.51. Coating adherence is extremely sensitive to the timing and method of cleaning, and possibly, therefore, to wet/dry cycles in soils and other seasonal and environmental factors. Finally, because even prolonged cleaning might not remove such a coating from natural

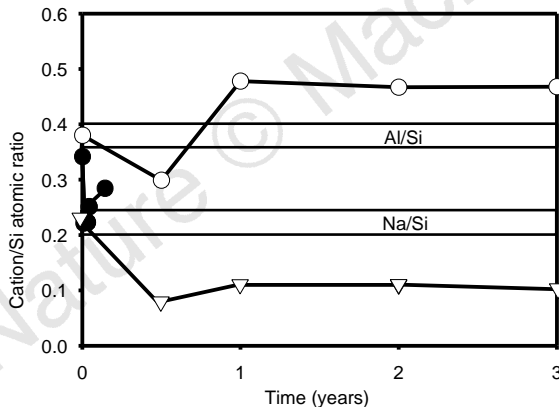


**Figure 3** Al/Si (empty circles) and Na/Si (empty triangles) atomic ratios for albite versus time of weathering, as measured by XPS. The boxes are defined by the high and low values of 11 Al/Si and Na/Si ratios measured on polished, unweathered albite blanks. We note that cleaning unweathered samples with and without a rinsing in water during polishing resulted in indistinguishable Al/Si values. All samples were placed in a ultraviolet ozone cleaning chamber<sup>28</sup> for ~30 min to remove adventitious carbon, then Al 2p, Si 2p and Na KLL peaks were measured using a Kratos Analytical XSAM 800pci instrument. The atomic % Al ranges from 7.1 to 7.9 for unweathered samples, and is 4.2, 7.6, 7.2 and 9.5, for samples weathered for 6 months, 1, 2 and 3 years, respectively. The atomic % Na ranges from 3.9 to 5.2 for unweathered samples, but is never higher than 2.6 during weathering. The atomic % Si ranges from 18.1 to 21.6 in unweathered samples. After weathering, the atomic % Si is 26.4, 17.5, 17.3 and 20.2 at 6 months, 1, 2 and 3 years, respectively. For comparison, XPS Al/Si atomic ratios<sup>10</sup> (filled circles) for Amelia Courthouse albite treated with pH 4 acetate/lithium-acetate buffer (25°C) laboratory solutions<sup>29</sup> are plotted. The rise in Al/Si with the duration of dissolution might be attributed to a back-reaction involving the development of an Al-rich surface coating similar to the one we observe on our naturally weathered samples.

samples, we suggest that a natural coating may explain previous observations<sup>3,4</sup> of Al enrichment on naturally weathered feldspars.

A simple mass balance based on minimum coating thickness and coverage and the minimum feldspar dissolution rate<sup>24</sup> shows that the coating contains more Al and Si than is liberated by feldspar dissolution, suggesting that the coating is at least partially derived from the soil pore waters. This argument is further strengthened by considering that the pore waters are supersaturated with respect to kaolinite (found in the coating) and that indigenous soil quartz grains in this feldspar-free soil also have an Al-, Si-rich coating, based on SEM-EDX.

Casey and others<sup>25</sup> have argued that the formation of secondary precipitates during weathering occurs by epitaxial growth on an Al-depleted, Si-enriched surface on silicate minerals. Our observations document for the first time, to our knowledge, that such a depleted layer may develop on naturally weathered samples. However, the lack of strong coating adherence before ageing further supports our suggestion that secondary phase formation occurs, in part, as silicic acid and aluminium ions precipitate from solution. Furthermore, our observation of an Al-depleted layer does not necessarily prove that this layer is needed for secondary mineral precipitation; indeed, our observations of aluminosilicate coatings on soil quartz grains suggests that epitaxial growth is not required for secondary precipitate formation.

On the basis of the development of dissolution textures (Fig. 1), feldspar dissolution occurs despite the presence of a patchy coating, and presumably, through the coating. For example, the 3.5-year sample, which probably had at least as much coating coverage as the 3-year sample (~35%) while buried, showed <<35% coverage under AFM after cleaning for 45 min. Yet, because both the 3- and 3.5-year samples showed dissolution texture everywhere, we infer some of these textured areas dissolved despite the presence of an overlying coating.

The coating may, however, partially inhibit dissolution, thus contributing to the laboratory/field-rate discrepancy. For example, stagnant pore waters in a feldspar-porewater-coating 'sandwich' may be more supersaturated with respect to albite than bulk soil pore water<sup>26</sup>. The lowered driving force for dissolution in such a microenvironment may partially explain the laboratory/field discrepancy, even if the  $\text{pH}_{\text{micropore}} < \text{pH}_{\text{porewater}}$ , as we might predict on the basis on experiments in which Al-rich coatings are precipitated<sup>27</sup>. We conclude that the laboratory and field dissolution mechanisms for feldspar are similar during early weathering, but that coating precipitation reactions may affect feldspar dissolution over geological timescales. □

Received 14 January; accepted 27 July 1998.

- Blum, A. & Stillings, L. in *Chemical Weathering Rates of Silicate Minerals* 291–352 (Mineralogical Society of America, Washington DC, 1995).
- White, A. in *Chemical Weathering Rates of Silicate Minerals* 407–462 (Mineralogical Society of America, Washington DC, 1995).
- Nesbitt, H. W. & Muir, I. SIMS depth profiles of weathered plagioclase and processes affecting dissolved Al and Si in some acidic soil solutions. *Nature* **334**, 336–338 (1988).
- Blum, A. E., White, A. F. & Hochella, M. F. The surface chemistry and topography of weathered feldspar surfaces. *Trans. Am. Geophys. Union, Abstr. Prog.* **73**, 602 (1992).
- Casey, W., Westrich, H. R. & Arnold, G. W. The surface chemistry of labradorite feldspar reacted with aqueous solutions at pH = 2, 3, and 12. *Geochim. Cosmochim. Acta* **52**, 2795–2807 (1988).
- Goossens, D. et al. A SIMS, XPS, SEM, TEM and FTIR study of feldspar surfaces after reacting with acidic solutions. *Proc. 6th Int. Symp. of Water-Rock Interaction* (ed. Miles, D. L.) 267–270 (Balkema, Rotterdam, 1989).
- Hellman, R., Eggleston, C. R., Hochella, M. F. & Crerar, D. A. The formation of leached layers on albite surfaces during dissolution under hydrothermal conditions. *Geochim. Cosmochim. Acta* **54**, 1267–1281 (1990).
- Muir, I., Bancroft, G. R. & Nesbitt, H. W. Characteristics of altered labradorite surfaces by SIMS and XPS. *Geochim. Cosmochim. Acta* **53**, 1235–1241 (1989).
- Muir, I., Bancroft, G. M., Shoty, W. & Nesbitt, H. W. A SIMS and XPS study of dissolving plagioclase. *Geochim. Cosmochim. Acta* **54**, 2247–2256 (1990).
- Rufe, E. *Influence of Surface Chemistry on the Natural and Artificial Weathering of Feldspars in the Soil Environment*. Thesis, Penn State Univ. (1994).
- Muir, I. & Nesbitt, H. W. Effects of aqueous cations on the dissolution of labradorite feldspar. *Geochim. Cosmochim. Acta* **55**, 3181–3189 (1991).
- Muir, I. & Nesbitt, H. W. Controls on differential leaching of calcium and aluminum from labradorite in dilute electrolyte solutions. *Geochim. Cosmochim. Acta* **56**, 3979–3985 (1992).
- Hochella, M. F., Ponder, H. B., Turner, A. M. & Harris, D. W. The complexity of mineral dissolution as viewed by high resolution scanning Auger microscopy: Labradorite under hydrothermal conditions. *Geochim. Cosmochim. Acta* **52**, 385–394 (1988).

14. Hellmann, R., Dran, J.-C. & Della Mea, G. The albite-water system: Part III. Characterization of leached and hydrogen-enriched layers formed at 300 °C using MeV ion beam techniques. *Geochim. Cosmochim. Acta* **61**, 1575–1594 (1997).
15. Casey, W., Westrich, H. R., Arnold, G. W. & Banfield, J. R. The surface chemistry of dissolving labradorite feldspar. *Geochim. Cosmochim. Acta* **58**, 821–832 (1989).
16. Chou, L. & Wollast, R. Steady state kinetics and dissolution mechanism of albite. *Am. J. Sci.* **285**, 963–993 (1985).
17. Brantley, S. & Stillings, L. Feldspar dissolution at 25 °C and low pH. *Am. J. Sci.* **296**, 101–127 (1996).
18. Blum, A. & Lasaga, A. Role of surface speciation in the low-temperature dissolution of minerals. *Nature* **331**, 431–433 (1988).
19. Lasaga, A. C. in *Chemical Weathering Rates of Silicate Minerals* 23–86 (Mineralogical Society of America, Washington DC, 1995).
20. Berner, R. A. & Holdren, G. R. Mechanism of feldspar weathering—II. Observations of feldspars from soils. *Geochim. Cosmochim. Acta* **43**, 1173–1186 (1979).
21. Holdren, G. R. & Berner, R. A. Mechanism of feldspar weathering—I. Experimental studies. *Geochim. Cosmochim. Acta* **43**, 1161–1171 (1979).
22. Lee, M. & Parsons, I. Microtextural controls of weathering of perthitic alkali feldspars. *Geochim. Cosmochim. Acta* **59**, 4465–4488 (1995).
23. Nugent, M. A., Maurice, P. A. & Brantley, S. L. in *Proc. 9th Int. Symp. of Water–Rock Interaction* (eds Arehart, G. B. & Hulston, J. R.) 387–390 (Balkema, Rotterdam, 1998).
24. Nugent, M. *Temporal Evolution of Feldspar Surfaces during the Initial Stages of in-situ Weathering*. Thesis, Penn State Univ. (1997).
25. Casey, W. H., Benfield, J. F., Westrich, H. R. & McLaughlin, L. What do dissolution experiments tell us about natural weathering? *Chem. Geol.* **105**, 1–15 (1993).
26. Hochella, M. F. & Banfield, J. F. in *Chemical Weathering Rates of Silicate Minerals* 353–406 (Mineralogical Society of America, Washington DC, 1995).
27. Violante, A., Gianfreda, L. & Violante, P. Effect of prolonged aging on the transformation of short-range ordered aluminum precipitation products formed in the presence of organic and inorganic ligands. *Clays Clay Miner.* **41**, 353–359 (1993).
28. Briggs, D. & Seah, M. P. *Practical Surface Analyses Vol. 1, Auger and X-ray Photoelectron Spectroscopy* (Wiley, New York, 1990).
29. Murphy, K. M. *Kinetics of Albite Dissolution: the Effect of Grain Size*. Thesis, Univ. Wyoming (1993).

**Acknowledgements.** We thank V. Bojan, D. Voigt, S. Yau, E. Rufe and B. Turner for discussions, M. Lee for feldspar TEM analyses, J. Hamilton for XPS analyses and Y. Chen and C. Doud for assistance with burial experiments. This work was funded by a grant from the Office of Basic Energy Sciences, Dept of Energy.

Correspondence and requests for materials should be addressed to M.A.N. (e-mail: nugent@sbmp04.ess.sunysb.edu).

## Evidence from the rare-earth-element record of mantle melting for cooling of the Tertiary Iceland plume

C. Tegner<sup>\*†</sup>, C. E. Lesher<sup>‡\*</sup>, L. M. Larsen<sup>\*§</sup> & W. S. Watt<sup>\*§</sup>

<sup>\*</sup> Danish Lithosphere Centre, Øster Voldgade 10, DK-1350 København K, Denmark

<sup>†</sup> Department of Earth Sciences, University of Aarhus, DK-8000 Aarhus C, Denmark

<sup>‡</sup> Department of Geology, University of California, Davis, California 95616, USA

<sup>§</sup> Geological Survey of Denmark and Greenland, Thoravej 8, DK-2400 København NV, Denmark

Widespread flood basalt volcanism and continental rifting in the northeast Atlantic in the early Tertiary period (~55 Myr ago) have been linked to the mantle plume now residing beneath Iceland<sup>1–5</sup>. Although much is known about the present-day Iceland plume<sup>6–9</sup>, its thermal structure, composition and position in the early Tertiary period remain unresolved. Estimates of its temperature, for example, range from >1,600 °C in some plume models<sup>3</sup> to ~1,500 °C based on the volume and composition of basaltic crust<sup>10–12</sup>. Several recent studies<sup>4</sup> have emphasized similarities in the thermal and chemical structure of the Tertiary and present-day plumes to argue for stability of the mantle anomaly, whereas others<sup>12,13</sup> relate variations in basalt volumes and compositions to changes in plume flux. Moreover, some authors<sup>1,2,13</sup> have assumed that the plume was rift-centred for its entire history, whereas others argue that it became ridge-centred only after plate separation<sup>4,15</sup>. Here we report compositional data for ~6,000 metres of flood basalts erupted in east Greenland, close to the inferred plume axis, that we use to constrain the Tertiary plume structure. Rare-earth-element systematics place limits on the

pressures and extents of mantle melting and show that the mantle was initially moderately hot (~1,500 °C), but that its temperature declined during flood volcanism. These observations are difficult to reconcile with current plume-head models, and call for important lithospheric control<sup>15,16–18</sup> on actively upwelling mantle along the rifted margin.

The east Greenland flood-basalt succession was emplaced in less than 1–2 Myr in the early Tertiary period<sup>19</sup>, and thickens southwards to >6 km towards the supposed hotspot track (Greenland–Iceland–Faeroes ridge; Fig. 1)<sup>20</sup>. Data on major- and rare-earth elements (REE) for a composite profile of the lava succession in the coastal mountains of the Sortebrae area (Fig. 1), totalling 331 flow units in four mappable formations<sup>20</sup>, are given in Fig. 2 (and in table form in Supplementary Information). Geochemically, these formations are composed of two distinct, uncontaminated (see Methods) suites; iron- and titanium-rich lavas (1.63–6.18 wt% TiO<sub>2</sub>) are found throughout, and low-Ti lavas (0.82–1.96 wt% TiO<sub>2</sub>) are restricted to the middle portion of the succession. The high-Ti suite has elevated chondrite-normalized<sup>21</sup> La/Sm<sub>N</sub> (1.09–2.11) and Dy/Yb<sub>N</sub> (1.18–1.62), while the low-Ti suite has near-chondritic to sub-chondritic REE ratios (La/Sm<sub>N</sub> = 0.42–0.94; Dy/Yb<sub>N</sub> = 0.99–1.14). Preliminary Sr–Nd isotope data for a subset of lavas confirm the highly depleted nature of the low-Ti suite and source (measured ε<sub>Nd</sub> = +8 to +11; <sup>87</sup>Sr/<sup>86</sup>Sr = 0.7026–0.7029) compared to that for the high-Ti suite (ε<sub>Nd</sub> = +5 to +8; <sup>87</sup>Sr/<sup>86</sup>Sr = 0.7030–0.7034; O. Stecher, unpublished data). In terms of major elements, REE and Sr–Nd isotopes, the low-Ti suite closely resembles depleted North Atlantic mid-ocean-ridge basalts (MORBs) formed by large-degree mantle melting (~15–25%; refs 22, 23) (Fig. 3a).

The systematic variations in REE ratios shown in Fig. 2 are most striking. In the lower portion of the succession (flow numbers 1–193; coded red circles) La/Sm<sub>N</sub> for the high-Ti suite increases up-section from ~1.2 to ~1.6, whereas the Dy/Yb<sub>N</sub> ratio decreases from ~1.6 to ~1.3 and correlates inversely with La/Sm<sub>N</sub> (Figs 2 and 3a). For the same stratigraphic interval, the variations in La/Sm<sub>N</sub> and Dy/Yb<sub>N</sub> for the low-Ti suite (yellow triangles) roughly parallel the high-Ti suite. In contrast, La/Sm<sub>N</sub> and Dy/Yb<sub>N</sub> for the high-Ti

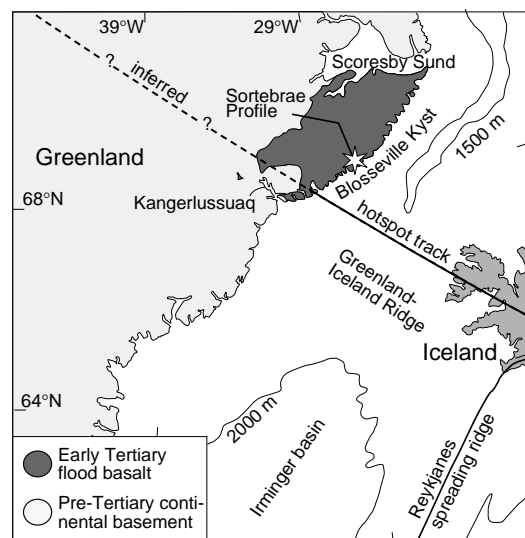


**Figure 1** Map of northeast Atlantic. Map showing exposed Tertiary flood basalt along the east Greenland volcanic rifted margin (~55 Myr old) and in Iceland (<16 Myr old), and ocean floor bathymetry. The solid line shows the track of the Iceland hotspot after continental breakup and the dashed line shows the inferred continuation of the plume track beneath Greenland<sup>14</sup>.